

# Monte Carlo Mean Field Treatment of Coherent Synchrotron Radiation Effects with Application to Microbunching Instability in Bunch Compressors

Gabriele Bassi

Department of Physics, University of Liverpool and the Cockcroft Institute, UK

Collaborators

Jim Ellison, Klaus Heinemann, Dept. of Math and Stats, University of New Mexico, Albuquerque, NM, USA

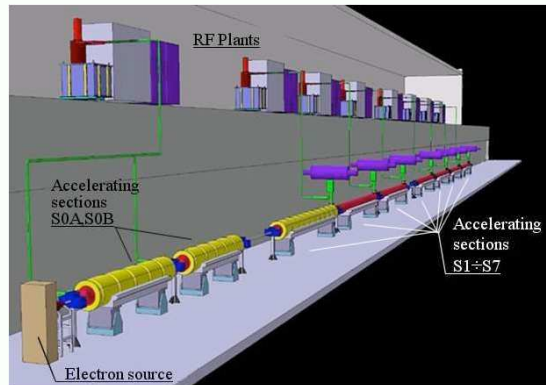
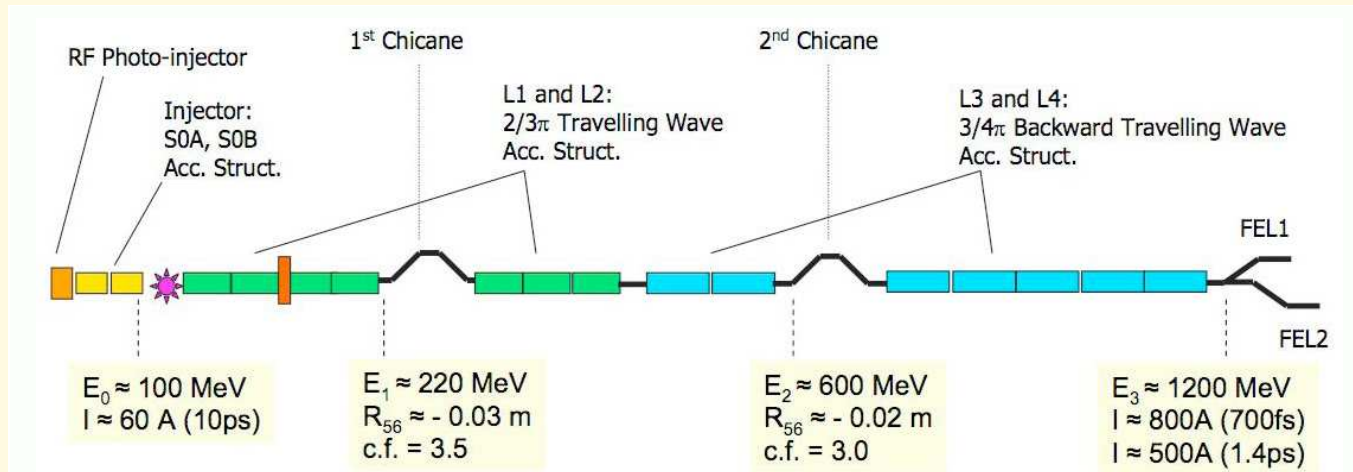
Robert Warnock, SLAC National Accelerator Laboratory, Menlo Park, CA, USA

1. Motivation
2. Coherent Synchrotron Radiation in Bunch Compressors
3. Self Consistent Vlasov-Maxwell Treatment in Lab Frame
4. Self Consistent Vlasov-Maxwell Treatment in Beam Frame
5. Beam to Lab Density Transformations
6. Field Calculation and Density Estimation
7. Microbunching Instability Studies for FERMI@Elettra
8. Discussion

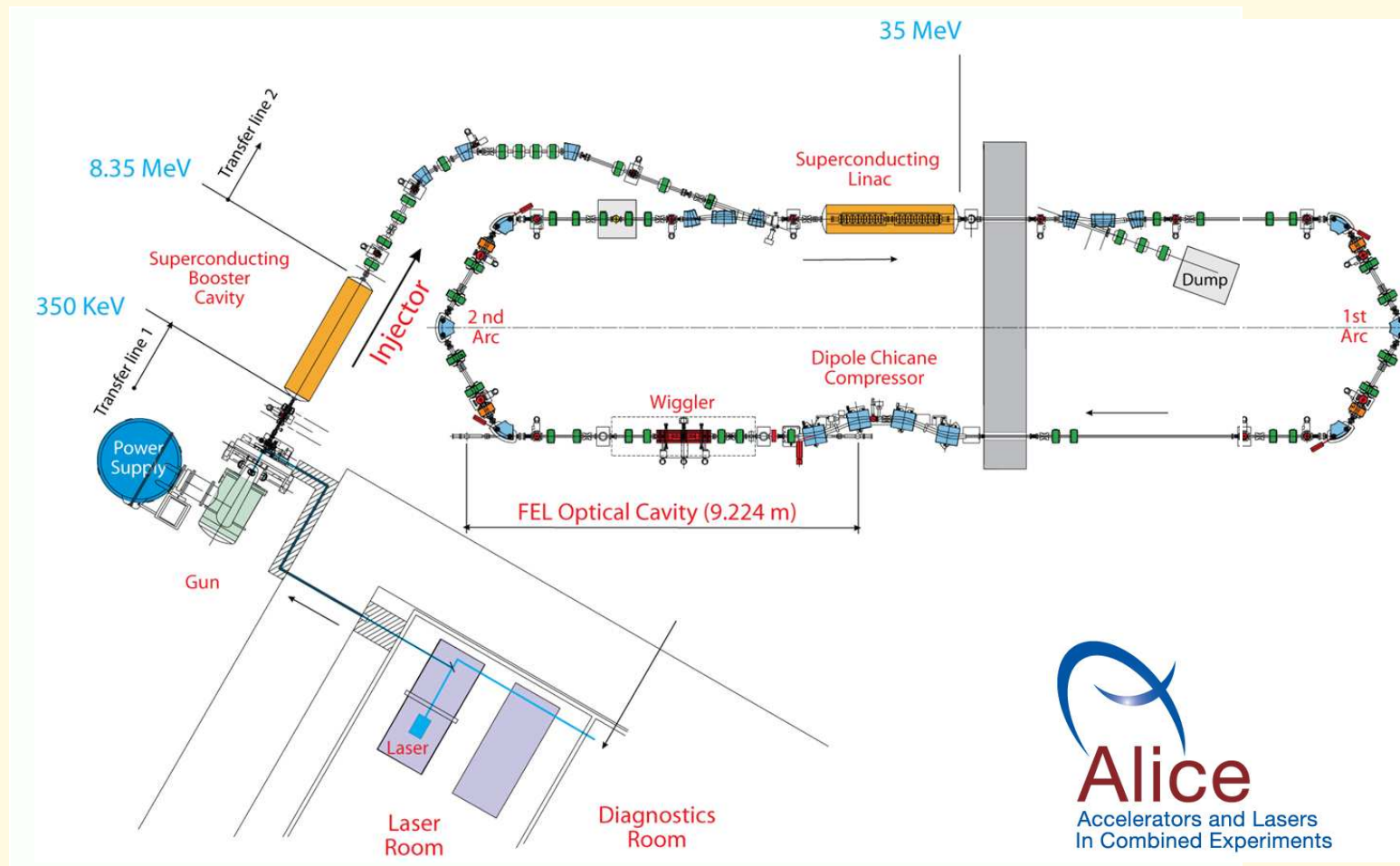
## Motivation

- Collective effects, such as coherent synchrotron radiation (CSR), can play a detrimental role on the beam quality and limit machine performance
- The need of high precision simulations of these effects requires state-of-the-art numerical techniques and high performance computing
- A system to study collective effects: 6D Vlasov-Maxwell system (models the particle beam as a non-neutral collisionless plasma)
- Its numerical integration is computationally too intensive
- A 4D Monte Carlo mean field approach has been developed and implemented on parallel high performance computer clusters
- We discuss its application to the study of the microbunching instability for the bunch compressor system of the FERMI@Elettra Free Electron Laser

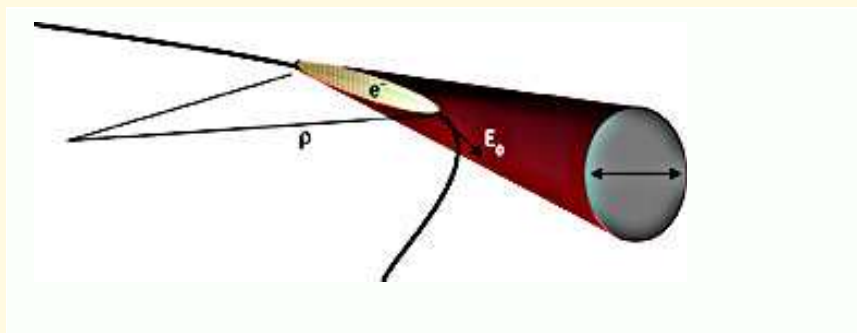
**FERMI@Elettra Free Electron Laser**



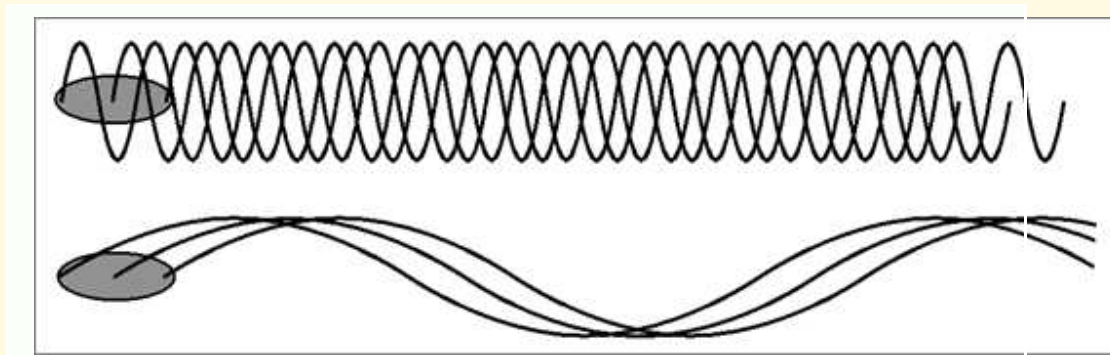
**ALICE Energy Recovery Linac**



## Coherent Synchrotron Radiation



Charged particles on a curved trajectory (bending magnet) emit synchrotron radiation

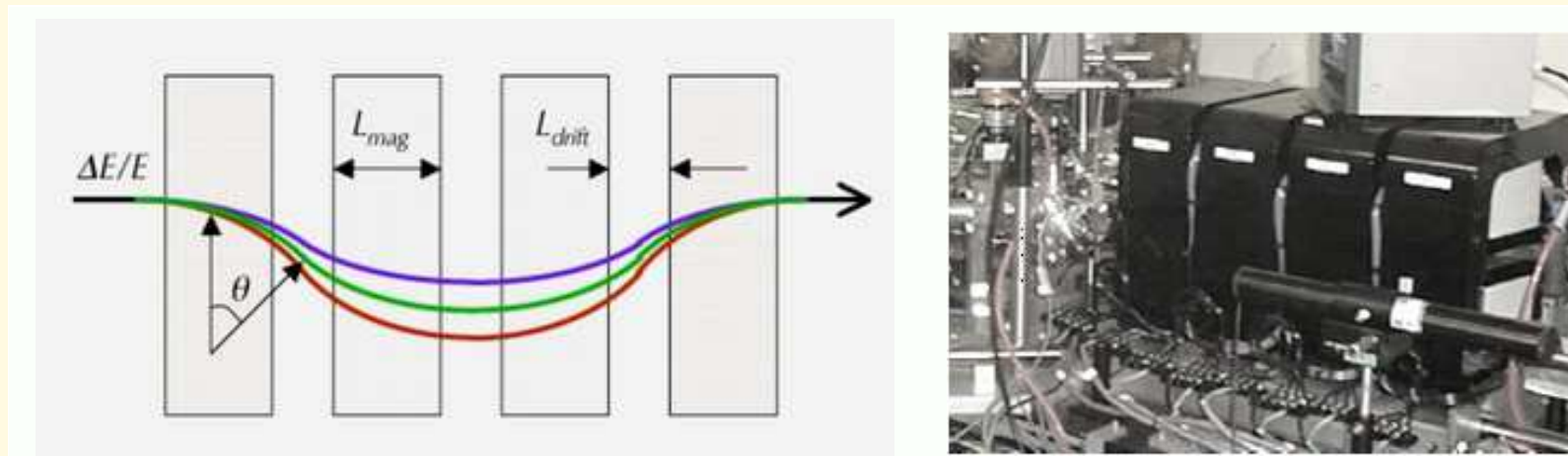


incoherent  $\lambda < \sigma_s$

coherent  $\lambda > \sigma_s$

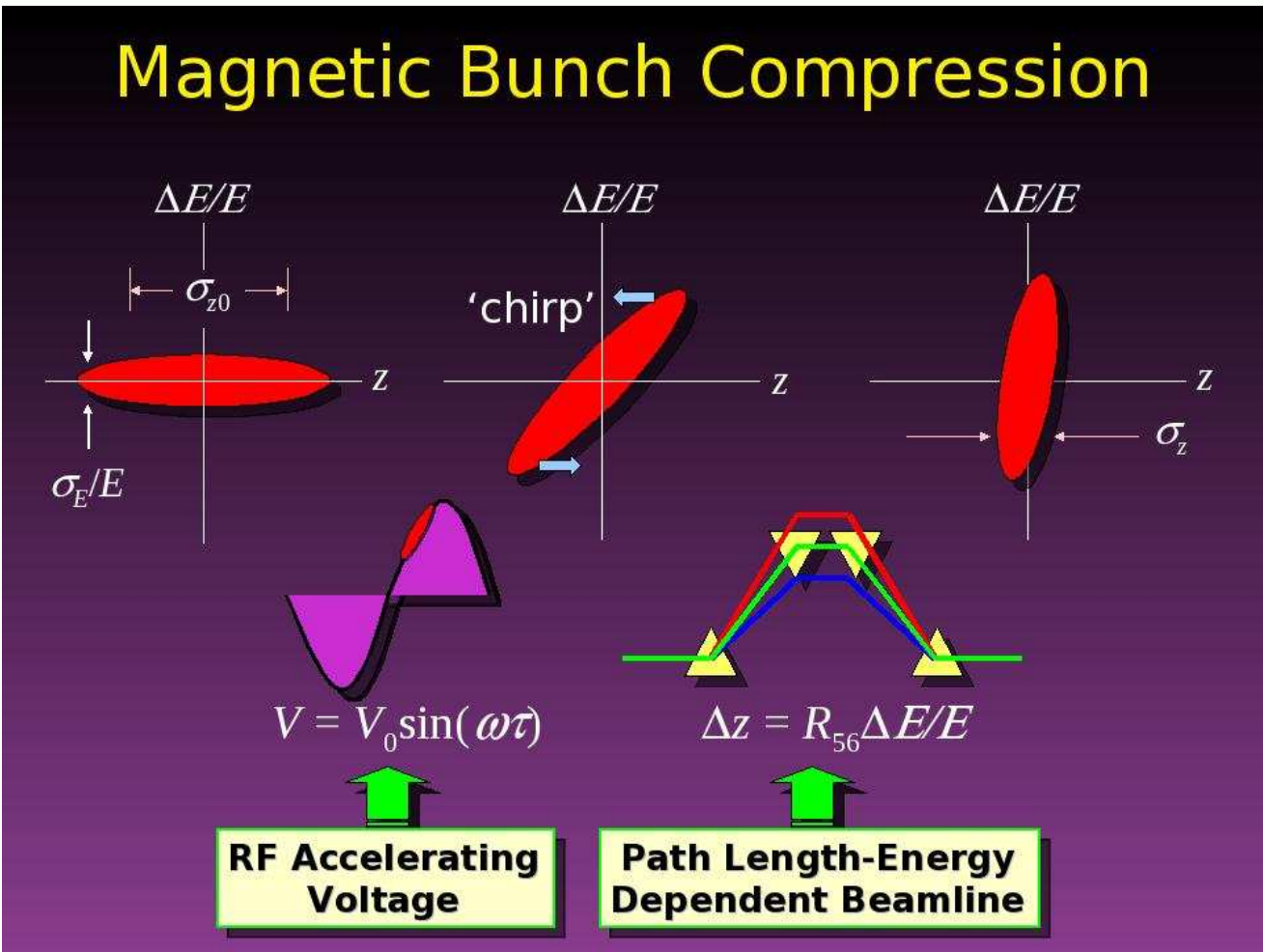
Synchrotron radiation is coherent (**CSR**) at wavelenghts  $\lambda$  longer than the bunch length  $\sigma_s$ .

If the bunch has microstructures, a coherent emission at wavelenghts shorter than the bunch length can lead to an instability (**microbunching instability**).

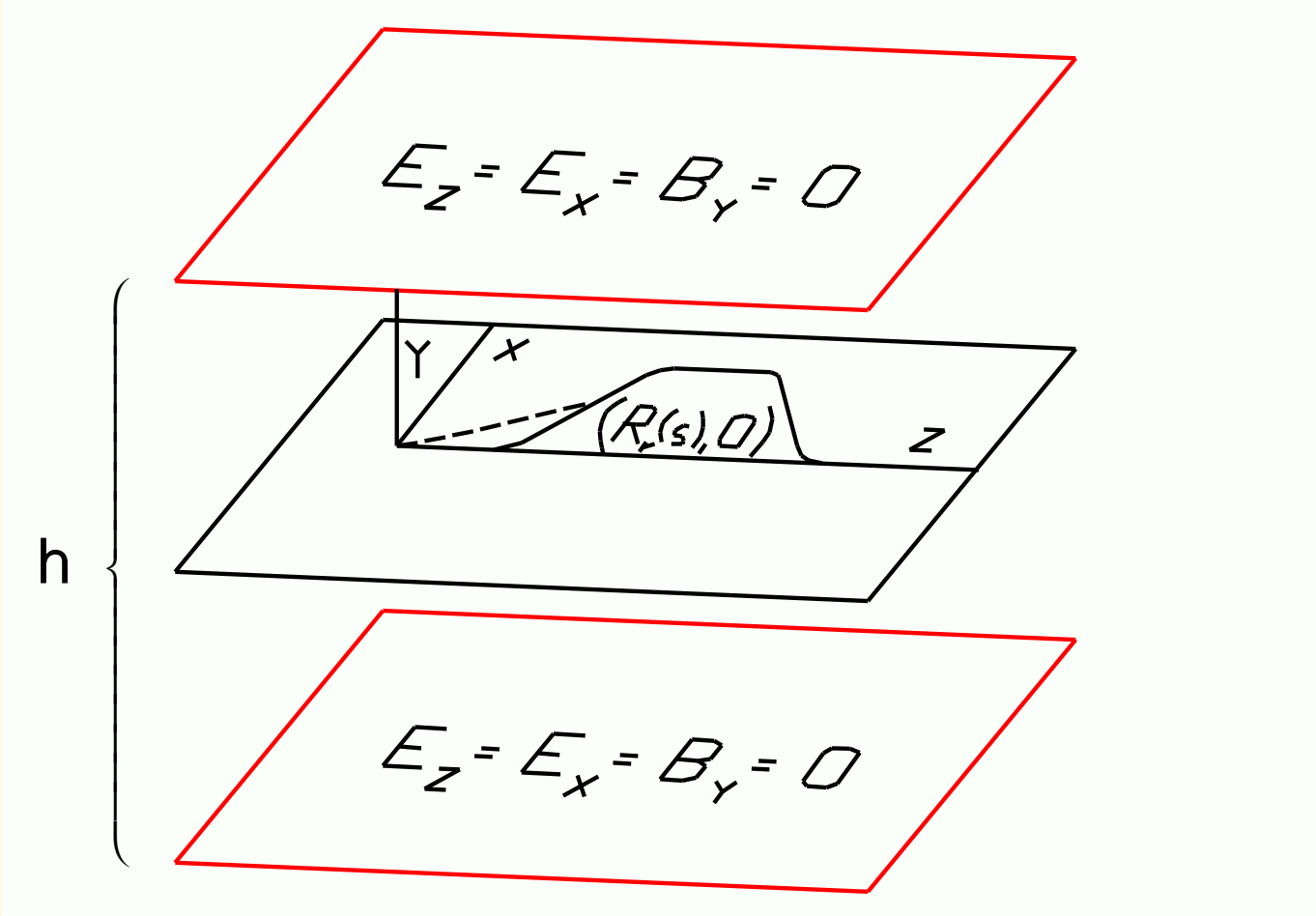
**Magnetic Bunch Compressor: 4-Dipole Chicane**

- Particles at higher energy move along shorter trajectory
- A proper correlation (called chirp) between energy and long. position is created in the linac before the chicane entrance, so that particles in the front of the bunch have less energy than particles in the tail
- This leads to bunch compression

**Magnetic Bunch Compressor System**



**Self Consistent Vlasov-Maxwell Treatment: Basic Lab Frame Setup**



## Self Consistent Vlasov-Maxwell Treatment for Sheet Beam in Lab Frame I

**Sheet Beam** model:  $f(Z, X, Y, P_Z, P_X, P_Y; u_0) = \delta(Y)\delta(P_Y)f_L(Z, X, P_Z, P_X; u_0)$ .

3D Wave equation (equivalent to Maxwell equations)

$$(\partial_Z^2 + \partial_X^2 + \partial_Y^2 - \partial_u^2)\mathcal{E} = \delta(Y)\mathbf{S}(\mathbf{R}, u), \quad \mathcal{E}(\mathbf{R}, Y = \pm g, u) = 0.$$

where  $u = ct$ ,  $\mathcal{E}(\mathbf{R}, Y, u) = (E_Z, E_X, B_Y)$ ,  $\mathbf{R} = (Z, X)^T$  and  $\dot{\phantom{a}} = d/du$ .

**Vlasov** equation (equation for the evolution of the average number of particles per unit volume for collisionless (uncorrelated) systems)

$$\partial_u f_L + \dot{\mathbf{R}} \cdot \partial_{\mathbf{R}} f_L + \dot{\mathbf{P}} \cdot \partial_{\mathbf{P}} f_L = 0, \quad f_L(\mathbf{R}, \mathbf{P}; u_i) = f_{L0}(\mathbf{R}, \mathbf{P})$$

where

$$\dot{\mathbf{R}} = \frac{\mathbf{P}}{m\gamma(P)c},$$

$$\dot{\mathbf{P}} = \frac{q}{c} \left[ \begin{pmatrix} E_Z(\mathbf{R}; u) \\ E_X(\mathbf{R}; u) \end{pmatrix} + \frac{[B_{ext}(Z) + B_Y(\mathbf{R}; u)]}{m\gamma(\mathbf{P})} \begin{pmatrix} P_X \\ -P_Z \end{pmatrix} \right].$$

and  $\mathbf{P} = (P_Z, P_X)^T$  and  $(E_Z(\mathbf{R}; u), E_X(\mathbf{R}; u), B_Y(\mathbf{R}; u)) \equiv \mathcal{E}(\mathbf{R}, 0; u)$ .

## Self Consistent Vlasov-Maxwell Treatment for Sheet Beam in Lab Frame II

Field Formula:

$$\mathcal{F}_L(\mathbf{R}; u) = -\frac{1}{4\pi} \sum_{k=-\infty}^{\infty} (-1)^k \int_{\mathbb{R}^2} d\mathbf{R}' \frac{\mathbf{S}(\mathbf{R}'; u - [|\mathbf{R}' - \mathbf{R}|^2 + (kh)^2]^{1/2})}{[|\mathbf{R}' - \mathbf{R}|^2 + (kh)^2]^{1/2}}.$$

where  $\mathcal{F}_L(\mathbf{R}; u) = (E_Z(\mathbf{R}; u), E_X(\mathbf{R}; u), B_Y(\mathbf{R}; u))$  and the source is

$$\mathbf{S}(\mathbf{R}; u) = Z_0 Q H(u - u_i) \begin{pmatrix} c\partial_Z \rho_L + \partial_u J_{L,Z} \\ c\partial_X \rho_L + \partial_u J_{L,X} \\ \partial_X J_{L,Z} - \partial_Z J_{L,X} \end{pmatrix},$$

where  $H$  is the unit step function.

The Vlasov equation and the self fields are coupled by  $Q\rho_L$  and  $Q\mathbf{J}_L$

$$\begin{aligned} \rho_L(\mathbf{R}; u) &= \int_{\mathbb{R}^2} d\mathbf{P} f_L(\mathbf{R}, \mathbf{P}; u), \\ \mathbf{J}_L(\mathbf{R}; u) &= \int_{\mathbb{R}^2} d\mathbf{P} (\mathbf{P}/m\gamma(\mathbf{P})) f_L(\mathbf{R}, \mathbf{P}; u). \end{aligned}$$

## Self Consistent Vlasov-Maxwell Treatment for Sheet Beam in Beam Frame I

Beam frame Frenet-Serret coordinates defined in terms of the reference orbit

$$\mathbf{R}_r(s) = (Z_r(s), X_r(s))^T \text{ in the } Y = 0 \text{ plane.}$$

Phase space transformation  $(\mathbf{R}, \mathbf{P}; u) \rightarrow (s, x, p_s, p_x; u)$

$$\mathbf{R} = \mathbf{R}_r(s) + xn(s), \quad \mathbf{P} = P_r(p_s \mathbf{t}(s) + p_x \mathbf{n}(s)).$$

Lab to beam transformation steps

$$(\mathbf{R}, \mathbf{P}; u) \rightarrow (s, x, p_s, p_x; u) \rightarrow (u, x, p_s, p_x; s) \rightarrow (z, x, p_z, p_x; s),$$

where  $z := s - \beta_r u$  and  $p_z := (\gamma - \gamma_r)/\gamma_r$ .

Exact relation between lab,  $f_L$ , and beam,  $f_B$ , phase space densities

$$f_B(\mathbf{r}, \mathbf{p}; s) = \frac{P_r^2}{\beta_r^2} f_L\{\mathbf{R}_r(s) + xn(s), P_r[p_s(\mathbf{p})\mathbf{t}(s) + p_x \mathbf{n}(s)]; (s - z)/\beta_r\}.$$

## Self Consistent Vlasov-Maxwell Treatment for Sheet Beam in Beam Frame II

Approximate beam frame equations of motion

$$\begin{aligned} z' &= -\kappa(s)x, & p'_z &= F_{z1}(z, x; s) + p_z F_{z2}(z, x; s), \\ x' &= p_x, & p'_x &= \kappa(s)p_z + F_x(z, x; s), \end{aligned}$$

where the self forces are

$$\begin{aligned} F_{z1} &= \frac{q}{P_r c} \mathbf{E}_{\parallel}(\mathbf{R}(s, x); \frac{s-z}{\beta_r}) \cdot \mathbf{t}(s), & F_{z2} &= \frac{q}{P_r c} \mathbf{E}_{\parallel}(\mathbf{R}(s, x); \frac{s-z}{\beta_r}) \cdot \mathbf{n}(s), \\ F_x &= \frac{q}{P_r c} \left[ \mathbf{E}_{\parallel}(\mathbf{R}(s, x); \frac{s-z}{\beta_r}) \cdot \mathbf{n}(s) - cB_Y(\mathbf{R}(s, x); \frac{s-z}{\beta_r}) \right]. \end{aligned}$$

Associated Vlasov IVP for the evolution of the beam frame phase space density

$$\partial_s f_B + \mathbf{r}' \cdot \nabla_{\mathbf{r}} f_B + \mathbf{p}' \cdot \nabla_{\mathbf{p}} f_B = 0, \quad f_B(\mathbf{r}, \mathbf{p}; 0) =: f_{B0}(\mathbf{r}, \mathbf{p}).$$

## Beam to Lab Density Transformations

- To solve Maxwell equations in lab frame must express lab frame charge/current density in terms of beam frame phase space density
- To a very good approximation

$$\rho_B(\mathbf{r}; s) \approx \rho_L(\mathbf{R}_r(s) + x\mathbf{n}(s); (s - z)/\beta_r),$$

thus

$$\rho_L(\mathbf{R}; u) \approx \rho_B(s(\mathbf{R}) - \beta_r u, x(\mathbf{R}); s(\mathbf{R})).$$

Replacing  $s$  by  $\beta_r u + z$  and expanding in  $z$  gives  $\rho_L(\mathbf{R}_r(\beta_r u) + M(\beta_r u)\mathbf{r}; u) \approx \rho_B(\mathbf{r}; \beta_r u + z)$ , where  $M(s) = [\mathbf{t}(s), \mathbf{n}(s)]$ . Finally, inverting (similarly for  $\mathbf{J}_L$ )

$$\begin{aligned} \rho_L(\mathbf{R}; u) &\approx \rho_B( M^T(\beta_r u)[\mathbf{R} - \mathbf{R}_r(\beta_r u)]; \beta_r u), \\ \mathbf{J}_L(\mathbf{R}; u) &\approx \beta_r c [\rho_B( M^T(\beta_r u)[\mathbf{R} - \mathbf{R}_r(\beta_r u)]; \beta_r u) \mathbf{t}(\beta_r u) \\ &\quad + \tau_B( M^T(\beta_r u)[\mathbf{R} - \mathbf{R}_r(\beta_r u)]; \beta_r u) \mathbf{n}(\beta_r u)]. \end{aligned}$$

where  $\tau_B(z, x; s) := \int p_x f_B(z, x, p_z, p_x; s) dp_z dp_x$ .

## Fields in Terms of Beam Frame Density and Causality Issue

To solve the beam frame equations of motion we need (ignoring shielding)

$$\mathcal{F}_L(\mathbf{R}_r(s) + x\mathbf{n}(s); (s-z)/\beta_r) = - \int_{\mathbb{R}^2} d\mathbf{R}' \frac{\mathbf{S}[\mathbf{R}'; (s-z)/\beta_r - |\mathbf{R}' - (\mathbf{R}_r(s) + x\mathbf{n}(s))|]}{4\pi |\mathbf{R}' - (\mathbf{R}_r(s) + x\mathbf{n}(s))|}$$

To compute this we need  $\rho_L[\mathbf{R}'; (s-z)/\beta_r - |\mathbf{R}' - (\mathbf{R}_r(s) + x\mathbf{n}(s))|]$ , as  $\mathbf{R}'$  varies over the support of  $\rho_L$  in  $\mathbb{R}^2$ , given  $\rho_B(\cdot; s')$  for  $0 \leq s' \leq s$ .

There is a causality issue here, since the calculation of  $\rho_L$  requires values  $\rho_B$  for  $s'$  slightly outside the range  $0 \leq s' \leq s$ .

This issue can be easily resolved with the following **slowing varying approximation**

$$f_B(\mathbf{r}, \mathbf{p}; s) \approx f_B(\mathbf{r}, \mathbf{p}; s + \Delta)$$

where  $\Delta$  is of the order of the bunch size.

### Field Calculation: Polar Coordinates

- Transform to polar coordinates  $(\chi, \theta)$ , and then take the temporal argument  $v$  in place of the radial coordinate  $\chi$ : make the transformation  $\mathbf{R}' \rightarrow (\theta, v)$  via

$$\mathbf{R}' = \mathbf{R} + \chi \mathbf{e}(\theta), \quad \mathbf{e}(\theta) = (\cos \theta, \sin \theta)^T, \quad v = u - \sqrt{\chi^2 + (kh)^2}$$

This conveniently removes the integrable singularity, giving the field simply as an integral over the source (ignoring shielding)

$$\mathcal{F}_L(\mathbf{R}_r(s) + M(s)\mathbf{r}, s/\beta_r) = -\frac{1}{4\pi} \int_{u_i}^{s/\beta_r} dv \int_{\theta_m}^{\theta_M} d\theta \mathbf{S}[\tilde{\mathbf{R}}(\theta, v; \mathbf{r}, s), v],$$

where  $\tilde{\mathbf{R}}(\theta, v; \mathbf{r}, s) = \mathbf{R}_r(s) + M(s)\mathbf{r} + (s/\beta_r - v)\mathbf{e}(\theta)$ .

- $\theta$  integration: **superconvergent** trapezoidal rule (localization in  $\theta$  for  $v \ll s/\beta_r$ )
- $v$  integration: **adaptive** Gauss-Kronrod rule (non uniform behavior in  $v$ )

The computational effort is  $O(N_z N_x N_v N_\theta)$ , where  $N_z$  and  $N_x$  are the number of grid points in  $z$  and  $x$  respectively,  $N_v$  is the number of evaluations for the  $v$  integration, and  $N_\theta$  is the number of evaluations for the  $\theta$  integration.

For  $N_z = 1000$ ,  $N_x = 128$ ,  $N_v = N_\theta = 1000$ ,  $O(N_z N_x N_v N_\theta) = O(10^{12})$ .

## Density Estimation: Orthogonal Series Method

- From scattered beam frame points at  $s \rightarrow$  **smooth/global** lab frame charge/current density via a **2D** Fourier method.

**1D Example:** 1D orthogonal series estimator of  $f(x)$ ,  $x \in [0, 1]$

$$f_J(x) := \sum_{j=0}^J \theta_j \phi_j(x), \quad \theta_j = \int_0^1 \phi_j(x) f(x) dx, \quad \phi_0(x) = 1, \phi_j(x) = \sqrt{2} \cos(j\pi x), j = 1, 2, \dots$$

Since  $f(x)$  is a probability density ( $X, X_n$  random variables distributed via  $f$ )

$$\theta_j = E\{\phi_j(X)\}, \quad \text{thus from Monte Carlo a natural estimate is } \hat{\theta}_j := \frac{1}{N} \sum_{n=1}^N \phi_j(X_n)$$

- The computational effort is  $O(\mathcal{N} J_z J_x)$ , where  $\mathcal{N}$  is the number of simulated particles,  $J_z$  and  $J_x$  the number of Fourier coefficients in  $z$  and  $x$  respectively. For  $\mathcal{N} = 5 \times 10^8$ ,  $J_z = 150$  and  $J_x = 50$ ,  $O(\mathcal{N} J_z J_x) = O(10^{12})$ .

## Density Estimation: Search for Improvement

- Cloud in cell charge deposition followed by computation of the Fourier coefficients of the truncated Fourier series by a simple quadrature (**already implemented**).

The computational effort is  $O(\mathcal{N}) + O(N_z N_x J_z J_x)$ , where  $\mathcal{N}$  is the number of simulated particles,  $N_z$  and  $N_x$  are the number of grid points in  $z$  and  $x$  respectively, and  $J_z$  and  $J_x$  the number of Fourier coefficients in  $z$  and  $x$  respectively.

For  $N_z = 1000$ ,  $N_x = 128$ ,  $J_z = 150$  and  $J_x = 50$ ,  $O(N_z N_x J_z J_x) = O(10^9)$ .

- Kernel density estimation using standard kernels like bivariate Gaussians or bivariate compact support kernels (e.g. Epanechnikov kernels).

The computational effort is  $O(\mathcal{N} \tilde{N}_z \tilde{N}_x)$ , where  $\mathcal{N}$  is the number of simulated particles and  $\tilde{N}_z \tilde{N}_x$  is the number of grid points inside the circle of radius  $h$  (bandwidth) centered at the scattered particle position  $z, x$ .

For  $\mathcal{N} = 5 \times 10^8$  and  $\tilde{N}_z = \tilde{N}_x = 4$ ,  $O(\mathcal{N} \tilde{N}_z \tilde{N}_x) = O(10^{10})$ .

- Wavelets-denoising (G. Bassi, B. Terzić, PAC09)

## Interaction Picture

- **Interaction** picture to **isolate** CSR dynamics.

$$\text{From } F_z = F_x = 0 \implies \zeta = \Phi(s|0)\zeta_0$$

$$\therefore \zeta'_0 = \Phi(0|s)F, \quad F = (0, F_z, 0, F_x).$$

- In component form

$$\begin{aligned} z'_0 &= -R_{56}(s)F_z - D(s)F_x, & p'_{z0} &= F_z, \\ x'_0 &= (sD'(s) - D(s))F_z - sF_x, & p'_{x0} &= -D'(s)F_z + F_x, \end{aligned}$$

where  $D(s) = \int_0^s \kappa(\tau)d\tau$  and  $R_{56}(s) = -\int_0^s D(\tau)\kappa(\tau)d\tau$ .

Here the principal solution matrix is

$$\Phi(s|0) = \begin{pmatrix} 1 & R_{56}(s) & -D'(s) & D(s) - sD'(s) \\ 0 & 1 & 0 & 0 \\ 0 & D(s) & 1 & s \\ 0 & D'(s) & 0 & 1 \end{pmatrix}.$$

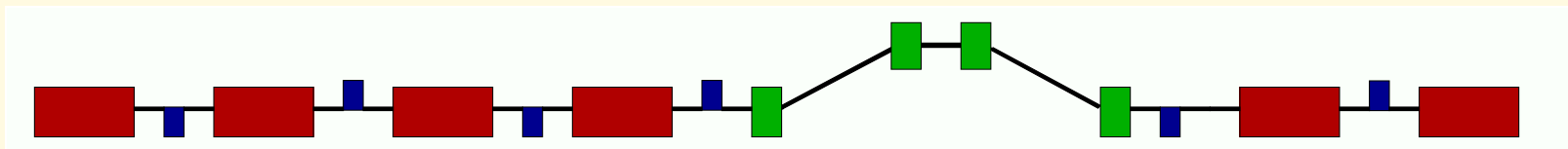
## Microbunching in FERMI@Elettra First Bunch Compressor

**Microbunching** can cause an instability which **degrades** beam quality, i.e. can cause an increase in energy spread and emittance

This is a major concern for free electron lasers where very bright electron beams are required

We discuss numerical results for the FERMI@Elettra first bunch compressor system. See G. Bassi, J.A. Ellison, K. Heinemann and R. Warnock, PRSTAB 12, 080704 (2009)

This system was proposed as a **benchmark** for testing codes at the first Workshop on Microbunching Instability held in Trieste in 2007



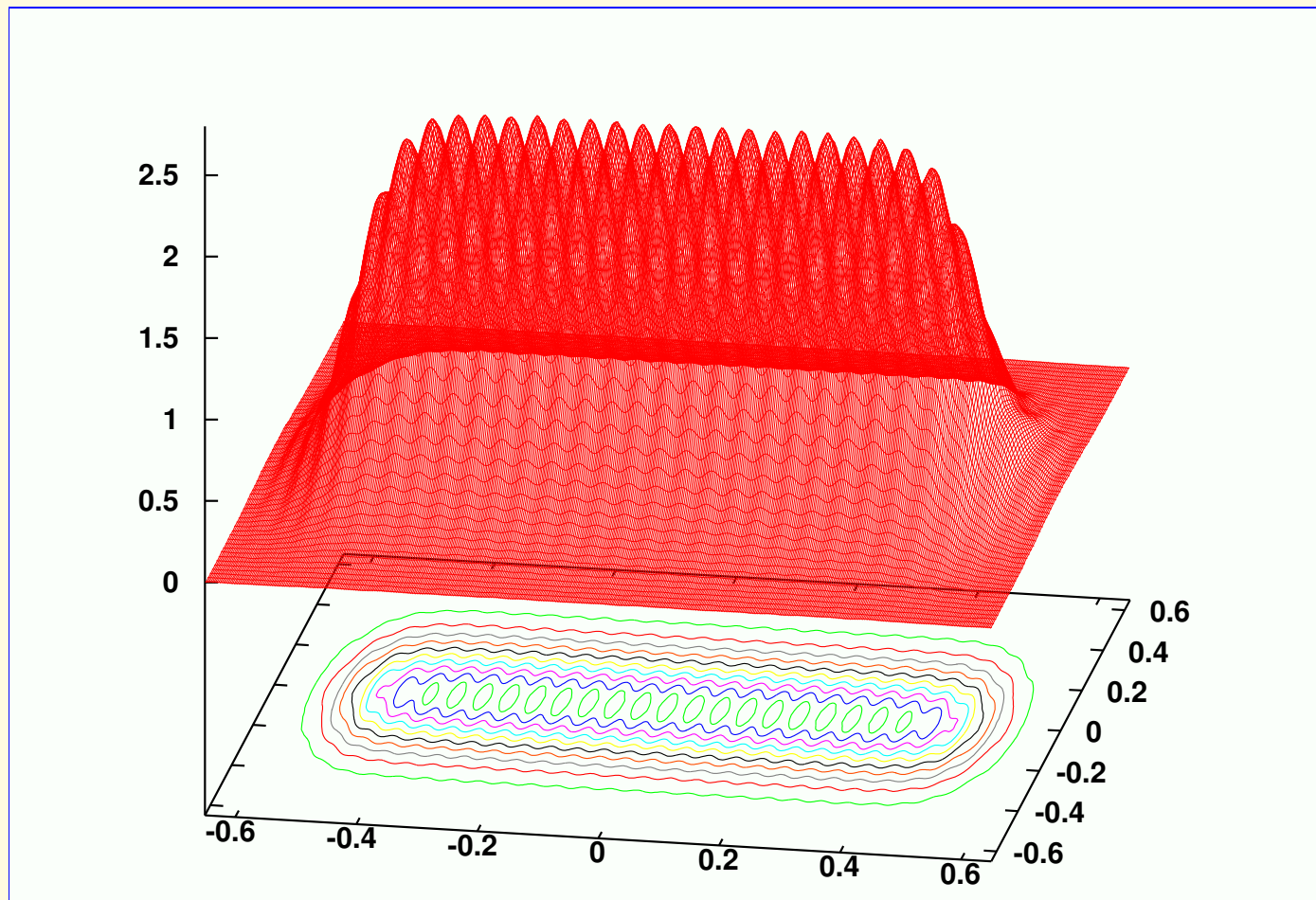
Layout first bunch compressor system

## FERMI@Elettra First Bunch Compressor Parameters

Table 1: Chicane parameters and beam parameters at first dipole

Parameter	Symbol	Value	Unit
Energy reference particle	$E_r$	233	MeV
Peak current	I	120	A
Bunch charge	Q	1	nC
Norm. transverse emittance	$\gamma\epsilon_0$	1	$\mu\text{m}$
Alpha function	$\alpha_0$	0	
Beta function	$\beta_0$	10	m
Linear energy chirp	h	-12.6	1/m
Uncorrelated energy spread	$\sigma_E$	2	KeV
Momentum compaction	$R_{56}$	0.057	m
Radius of curvature	$\rho_0$	5	m
Magnetic length	$L_b$	0.5	m
Distance 1st-2nd, 3rd-4th bend	$L_1$	2.5	m
Distance 2nd-3rd bend	$L_2$	1	m

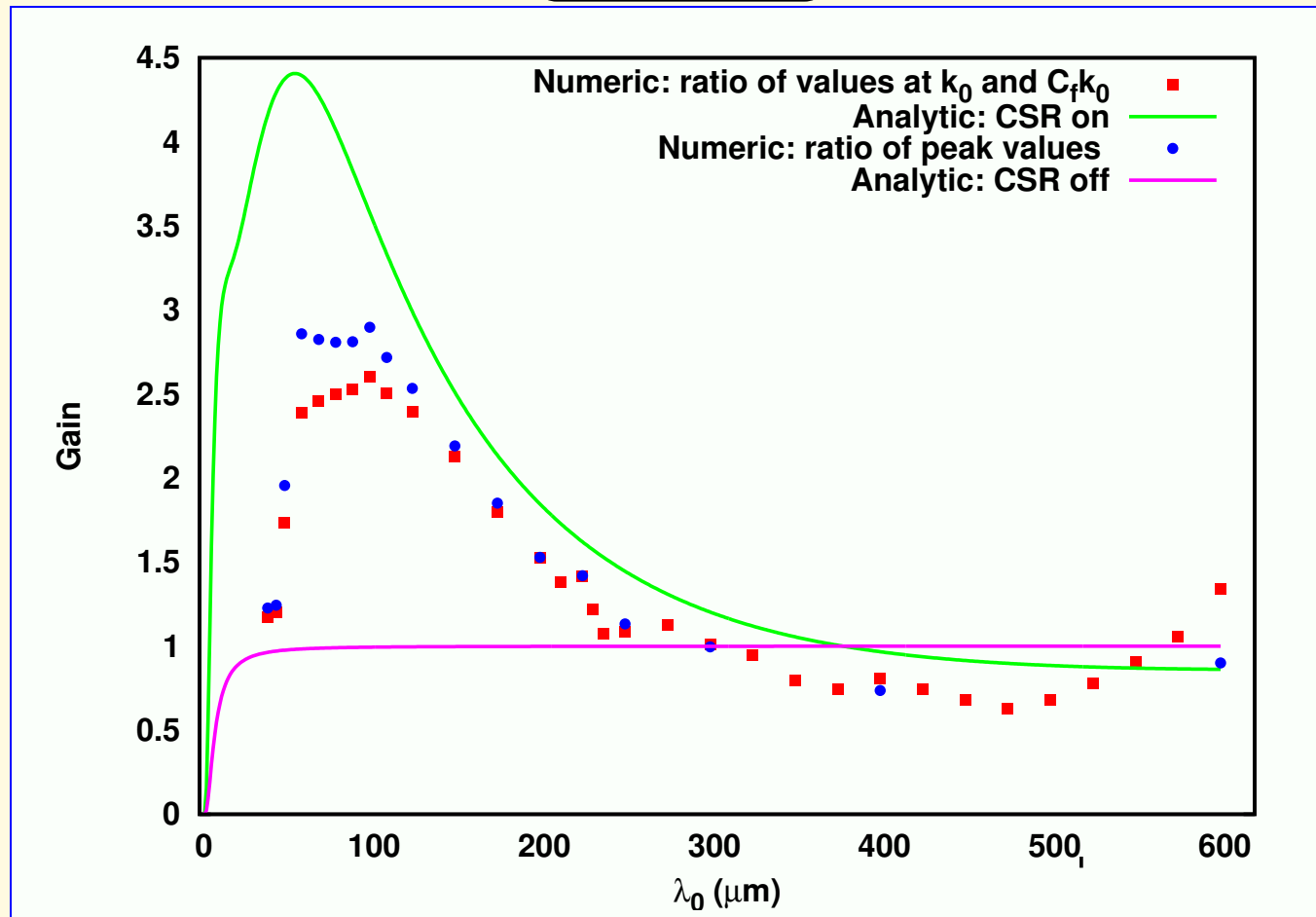
**Initial 2D Spatial Density**



Initial spatial density in grid coordinates for  $A=0.05$ ,  $\lambda_0 = 100\mu\text{m}$ .

Init. phase space density =  $(1 + A \cos(2\pi z / \lambda_0))\mu(z)\rho_c(p_z - hz)g(x, p_x)$ .

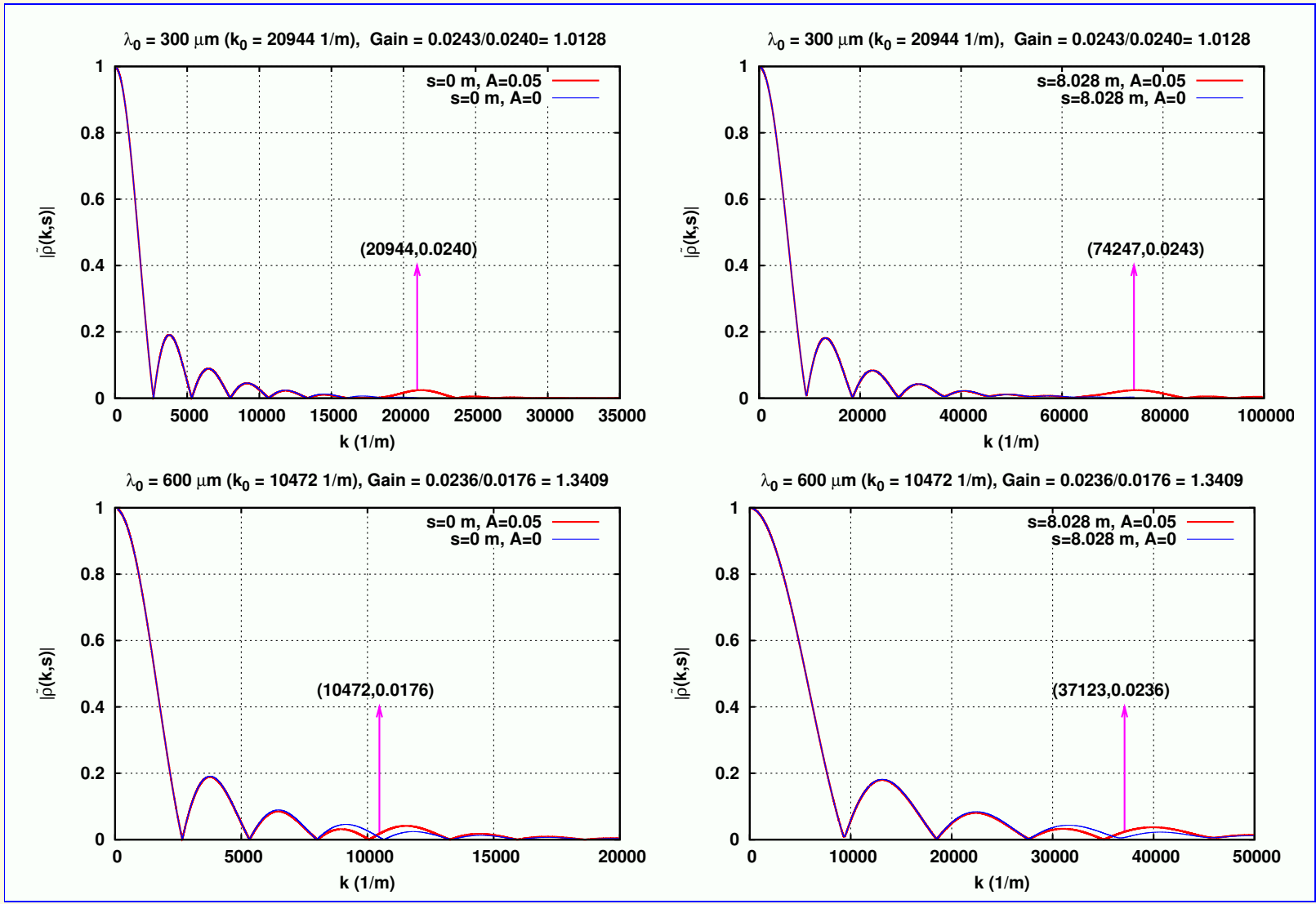
### Gain factor



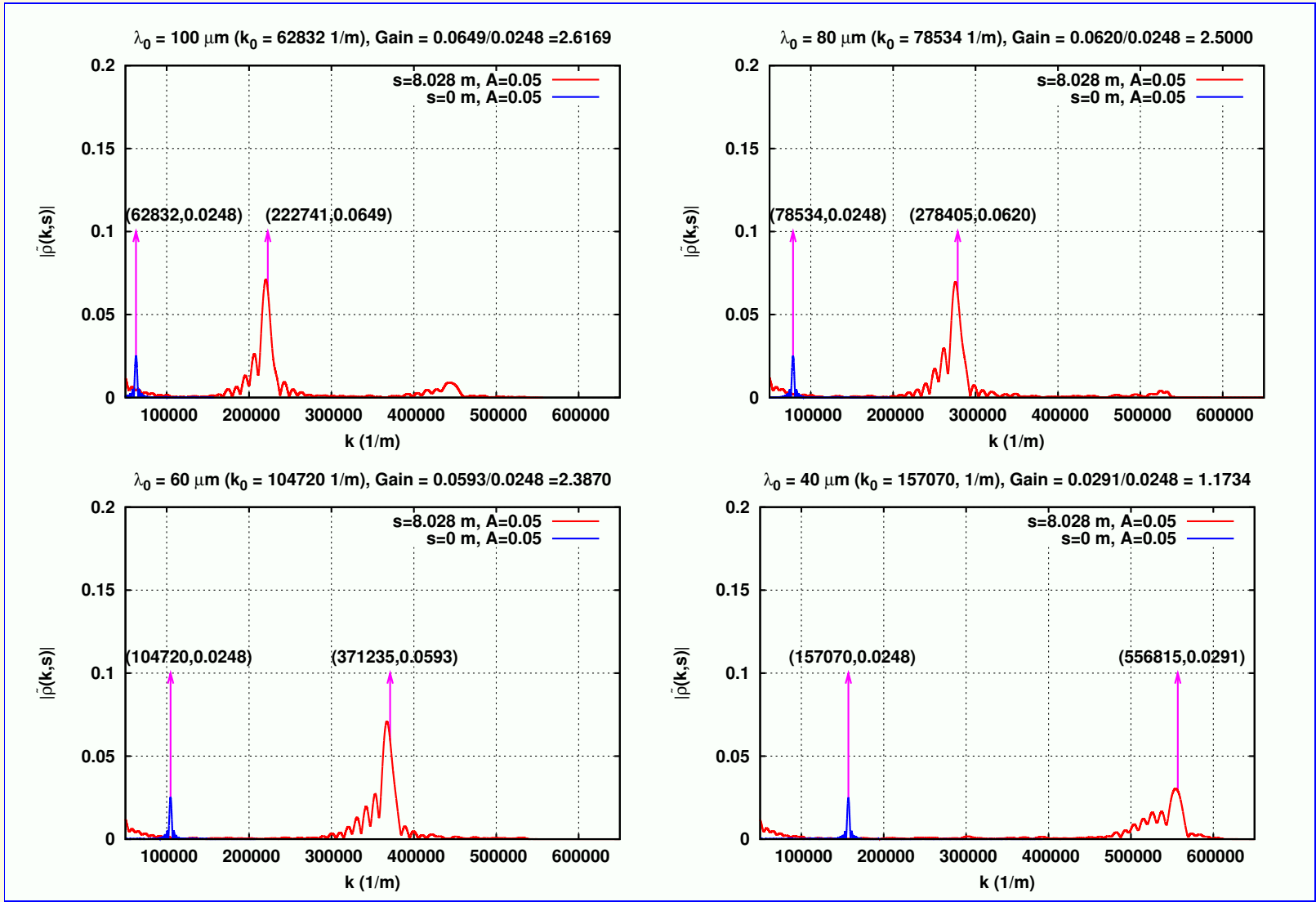
Gain :=  $|\tilde{\rho}(k_f, s_f)/\tilde{\rho}(k_0, 0)|$ ,  $\tilde{\rho}(k, s) = \int dz \exp(-ikz)\rho(z, s)$  and  $k_f = C(s_f)k_0$   
 for  $\lambda_0 = 2\pi/k_0$ . Here  $C(s_f) = 1/(1 + hR_{56}(s_f)) = 3.54$ ,  $s_f = 829\text{m}$ .

H. Huang and K. Kim, PRSTAB 5, 074401, 129903 (2002); S. Heifets, G. Stupakov and S. Krinsky, PRSTAB 5, 064401 (2009); G. Bassi, J.A. Ellison, K. Heinemann and R. Warnock, PRSTAB 12, 080704 (2009).

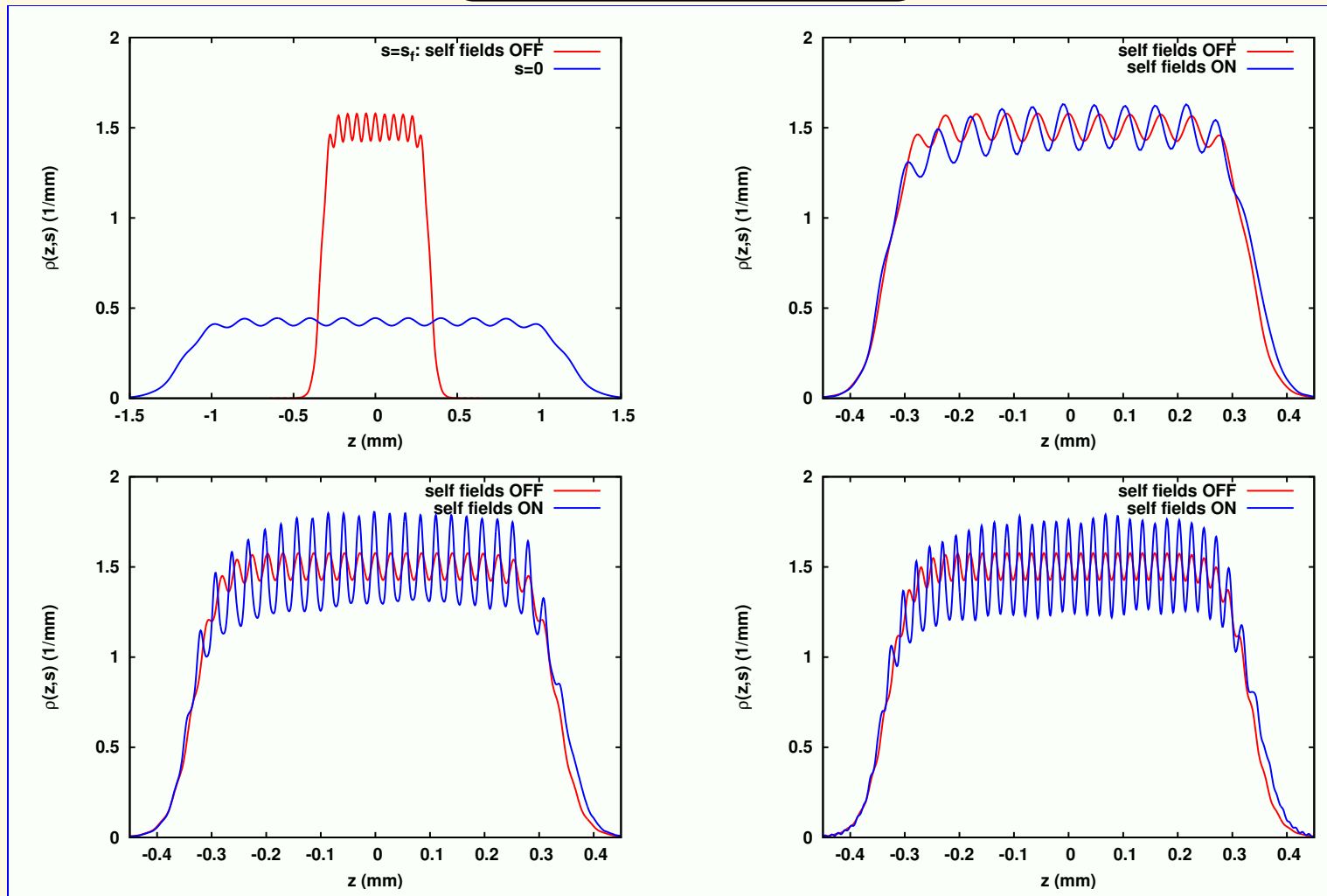
**Spectra Longitudinal Density I**



**Spectra Longitudinal Density II**



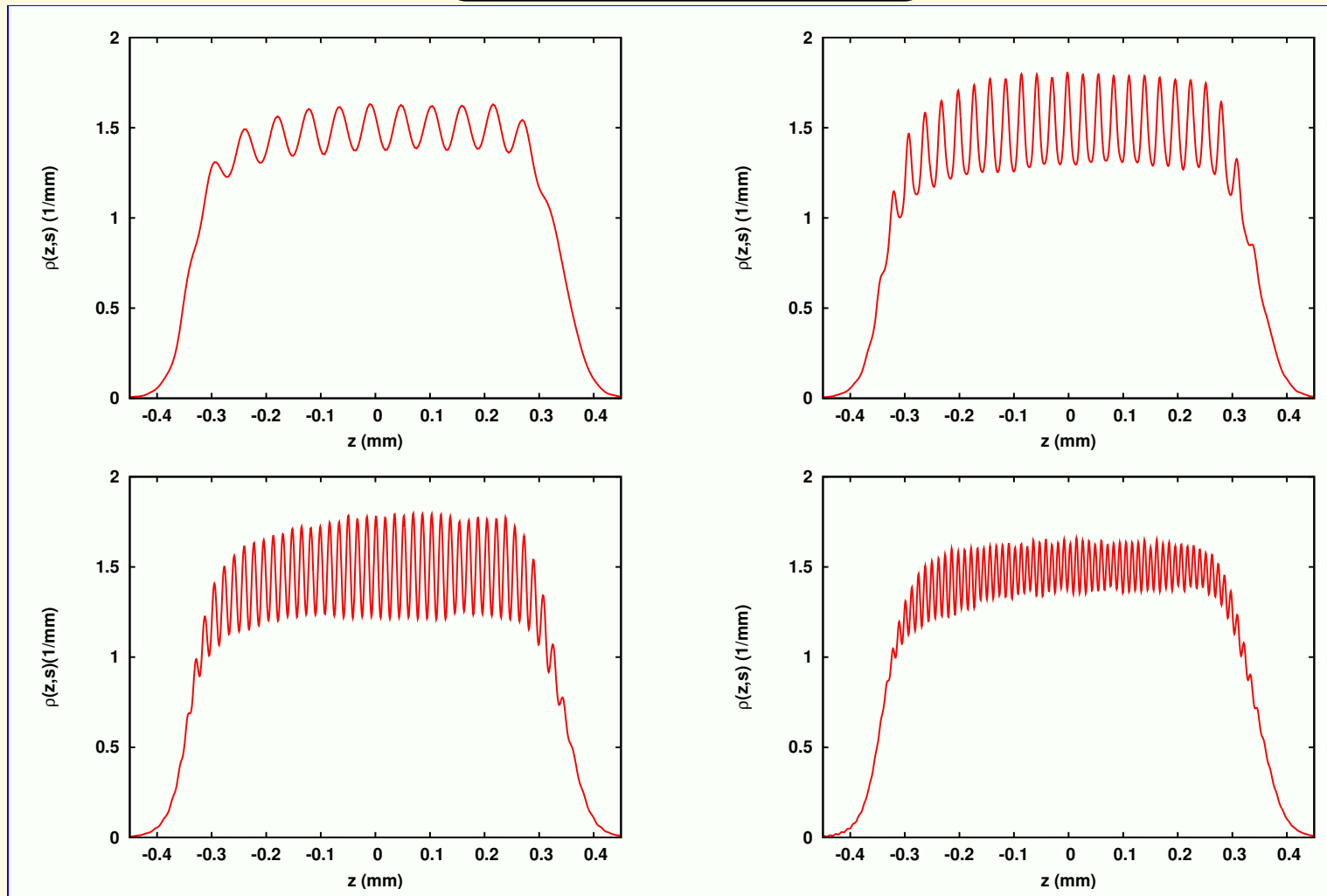
### Longitudinal Density I



$\lambda_0 = 200\mu\text{m}$  (top left),  
 $\lambda_0 = 100\mu\text{m}$  at  $s = s_f$  (bottom left),

$\lambda_0 = 200\mu\text{m}$  at  $s = s_f$  (top right),  
 $\lambda_0 = 80\mu\text{m}$  at  $s = s_f$  (bottom right).

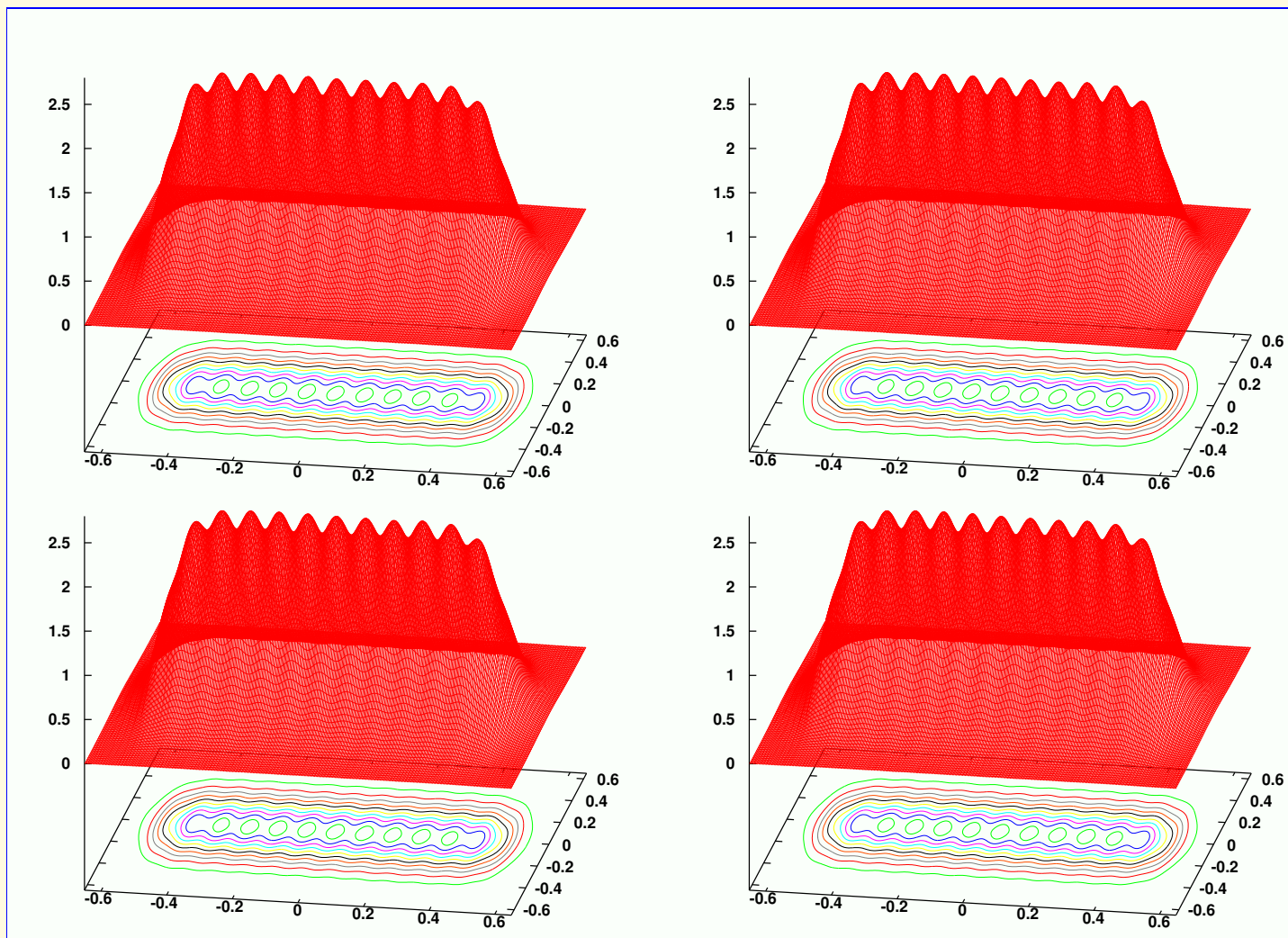
**Longitudinal Density II**



$\lambda_0 = 200 \mu\text{m}$  at  $s = s_f$  (top left),  
 $\lambda_0 = 60 \mu\text{m}$  at  $s = s_f$  (bottom left),

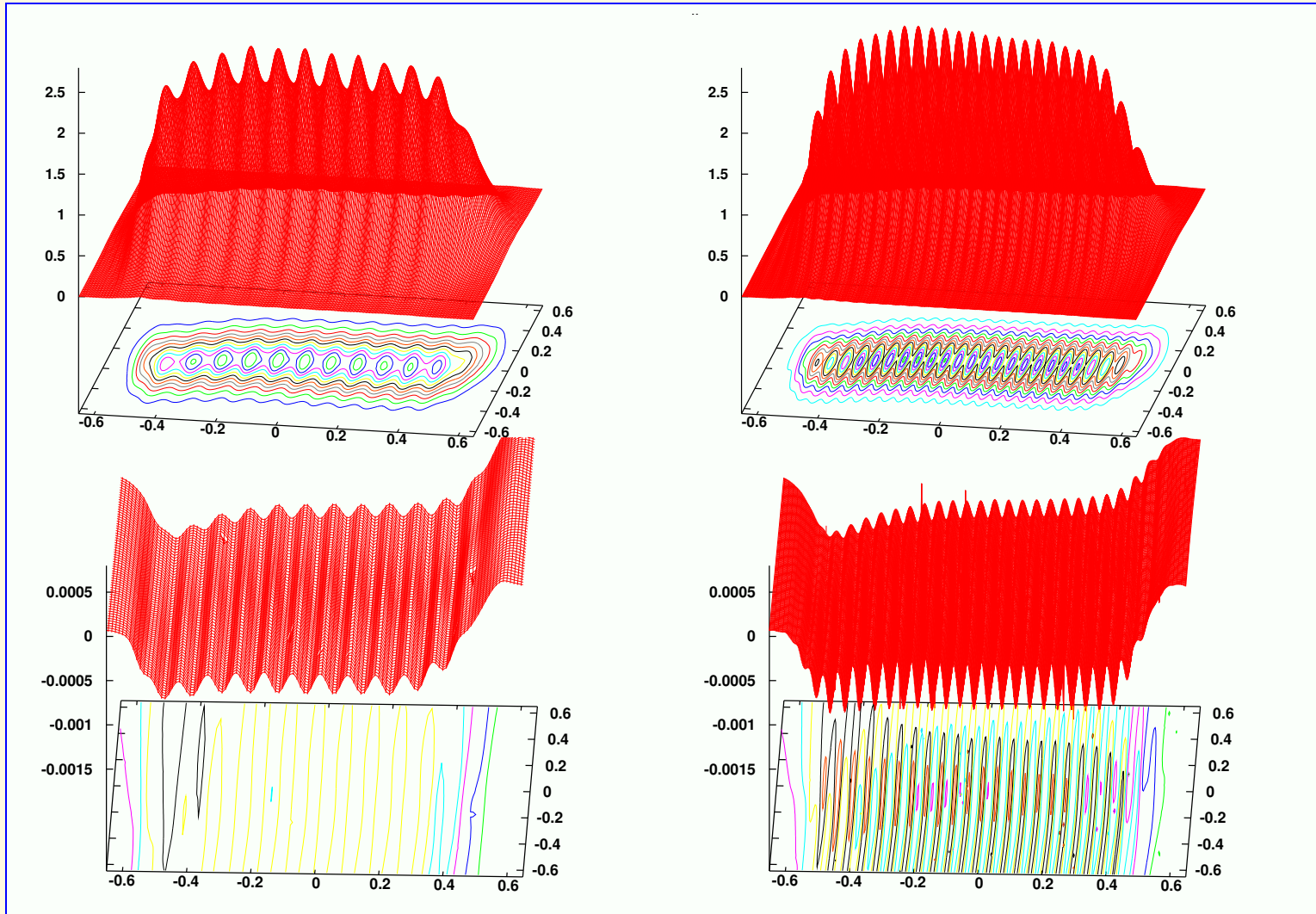
$\lambda_0 = 100 \mu\text{m}$  at  $s = s_f$  (top right),  
 $\lambda_0 = 40 \mu\text{m}$  at  $s = s_f$  (bottom right).

**Stationary Grid**



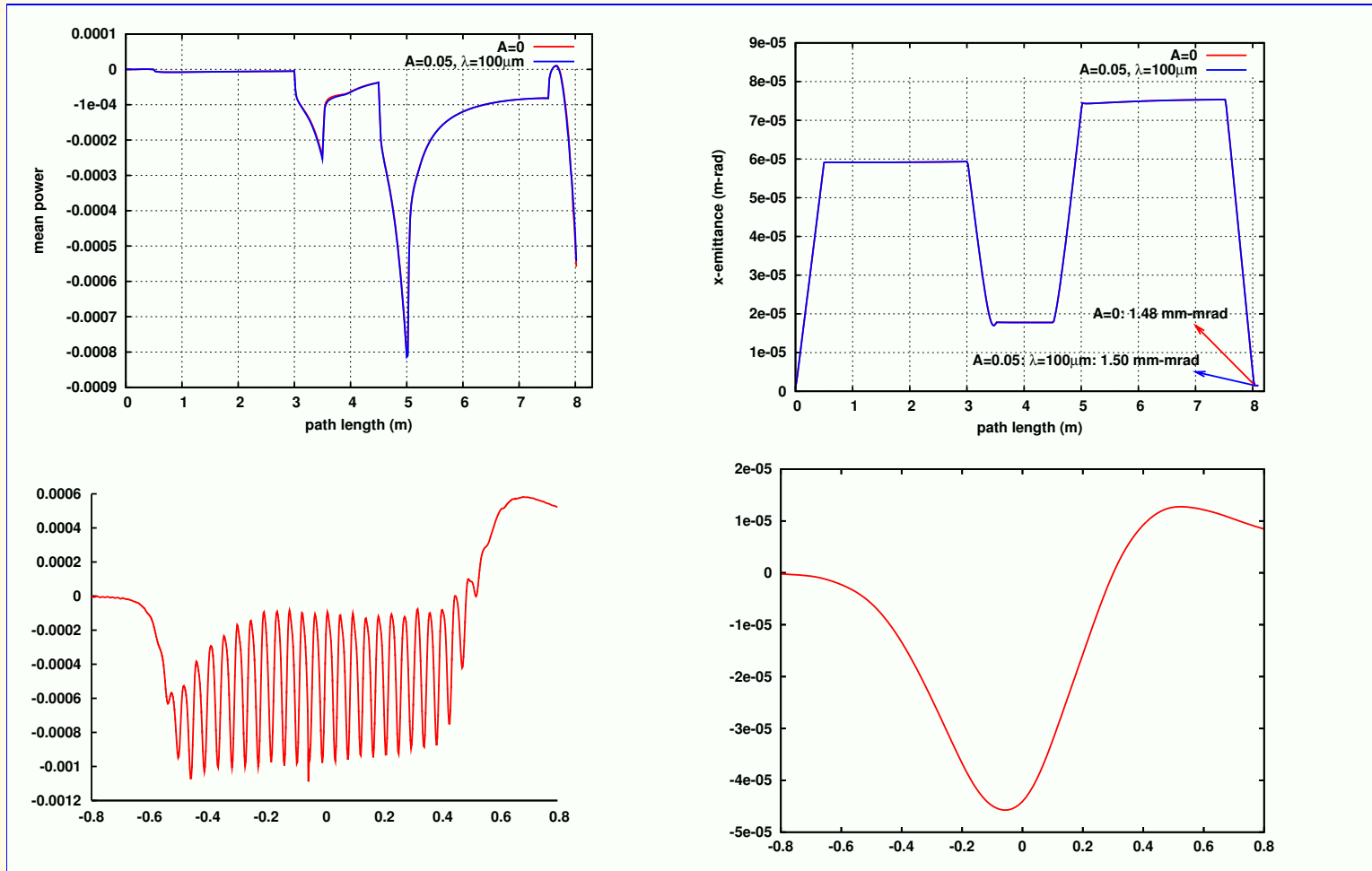
$\lambda_0=200\mu\text{m}$ .  $s=0.25s_f$  (top left),  $s=0.5s_f$  (top right),  $s=0.75s_f$  (bottom left),  $s=s_f$  (bottom right).

**2D spatial density and longitudinal force at  $s = s_f$**



$\lambda_0 = 200\mu\text{m}$  (top left),  $\lambda_0 = 100\mu\text{m}$  (top right),  $\lambda_0 = 200\mu\text{m}$  (bottom left),  $\lambda_0 = 100\mu\text{m}$  (bottom right)

**Mean Power, Transverse Emittance and 2D vs 1D longitudinal force**



Mean power (top left), transverse emittance (top right), 2D longitudinal force (section at  $x = 0$ ) at  $s = s_f$  (bottom left), 1D longitudinal force (steady state CSR wake) (bottom right).

## Discussion

- FERMI@Elettra microbunching studies at  $\lambda_0 \geq 40\mu\text{m}$ :
  - Very small effect of  $\mu$ BI on mean power and transverse emittance
  - Gain factor at long wavelengths shows breakdown coasting beam assumption
  - Gain factor at short wavelengths indicates deviations from analytical gain formula
- Work in progress and future work:
  - Study wavelengths shorter than  $\lambda_0 = 40\mu\text{m}$
  - Study dependence on the amplitude of the initial modulation and on the uncorrelated energy spread
  - Study initial perturbation with more than one frequency
  - Study energy modulations.

## Computational Issues

- Intensive memory requirement and expensive computational cost:
  - Typical simulations done on the parallel clusters ENCANTO in New Mexico and NERSC at LBNL: N procs = 200-1000, N particles =  $2 \times 10^7$ - $5 \times 10^8$ , few hours of CPU time
  - Memory requirement: for  $\lambda_0 = 50 \mu\text{m}$  store 3D array of dimension  $1500 \times 128 \times 200$  on master processor (to avoid massive communications between slave processors)
- To reduce storage/computational cost:
  - Analytical work + state of the art numerical techniques: integration, interpolation, density estimation
  - Parallel computing